

Combination of cooling and dust collection systems in a sulfuric acid plant: a cooling coil and a rotary drum with sprays

I. Aarab¹, M. Bennajah^{1*}, R. Elkacmi², M. Maalmi¹, L. N. Qadiri¹, R. Idchabani¹

1. Department of Process Engineering, National School of Mineral Industries of Rabat, BP 753 Agdal, Rabat, Morocco

2. Department of Chemistry and Valorisation, Faculty of Sciences Ain-Chock, HASSAN II University of Casablanca, BP 5366 Maarif, Casablanca, Morocco

Received 03 Nov 2016,
Revised 12 Mar 2017,
Accepted 17 Mar 2017

Keywords

- ✓ Roasting pyrrhotite;
- ✓ Dioxide sulfur;
- ✓ Hematite-rich waste;
- ✓ Dust;
- ✓ Spraying
- ✓ Cooling coil

M. Bennajah

bennajah.mounir@gmail.com
+212664860936

Abstract

The particularity of the roasting pyrrhotite process is the production of both dioxide sulfur and a hematite-rich waste Fe_2O_3 as a secondary product, known as roasted pyrrhotite ash. Because of its high temperature $270^\circ C$ and its ultrafine particles, the roasting processing generates excessive dust which could harm not only worker's health but also environment. The dust collection system in place in the case study plant (Morocco) consisting of cyclones and ESP precipitators do not collect all of this dust. To mitigate the spreading of dust all over the plant, an additional system to settle the dust is needed. In this work, we propose a combination of cooling and dust collecting systems at the same time, that ensures a decrease of high temperature, an obstacle while spraying, and then settle down airborne hematite. So, a cooling coil is immersed into the bed of fine particles of the conveyor moving towards the storage hall. After being cooled, the challenge is the capture of dust in a rotating drum provided with sprays.

Nomenclature

$T_{dust,out}$ outlet temperature of dust ($^\circ C$).	ρ_p dust density (Kg/m^3).
T_d temperature of dust ($^\circ C$).	μ_g viscosity of gas ($Kg/m.s$).
T_g temperature of gas ($^\circ C$).	λ_g thermal conductivity ($KW/m.K$).
Q_{global} overall exchanged heat (W).	ε bed porosity.
Q_i heat exchanged by the mechanism i(W).	ε_{mf} porosity at minimum fluidization.
U global exchange coefficient ($W/m^2.K$).	Re_{mf} Reynolds number at minimum fluidization velocity.
S_i exchange surface (m^2).	D_t diameter of the coil (mm).
$DTLM$ logarithmic temperature difference.	θ_s sphericity of particles.
\dot{m}_{dust} dust rate (Kg/h).	l length of contact between coil tubes and dust particles (m).
d_p particle diameter (μm).	U_g gas velocity(m/s).
h_p exchange coefficient particle-gas($W/m^2.K$).	T couple of equipment(Nm).
h_{conv} convective heat exchange coefficient ($W/m^2.K$).	n rotating velocity of drum(tr/min)
h_c heat exchange coefficient at hot side ($W/m^2.K$).	R drum radius (m).
h_f heat exchange coefficient at cold side($W/m^2.K$).	A, B empirical coefficient depending on filling rate f of drum, the break angle coefficient of powder ϕ and the friction coefficient at the wall μ_w .
ΔT variation of the temperature ($^\circ C$).	Ne Newton number.
n_{crit} critical velocity of rotating drum (tr/min).	Fr Froude number.
$C_{p,i}$ heat capacity ($KJ/Kg.K$).	S saturation rate of Newitt et Conway-Jones (1958).
a_p particle surface (m^2).	w mass ratio of the wetting liquid and solid particles(Kg/Kg)
Nu_p Nusselt number of dust.	ρ_l density of wettingliquid (Kg/m^3).

Pr_g Prandtl number of gas.	θ spray angle.
Re_p Reynolds number of dust (particles).	L distance covered by spraying (m).
Ar Archimede number.	b spray distance between nozzles and bed of particles (m).
ρ_g gas density (Kg/m ³).	

1. Introduction

In this case study (Moroccan plant), combustion of pyrrhotite Fe_7S_8 generates not only sulfur dioxide (used to produce sulfuric acid) but also the dust of hematite Fe_2O_3 according to the following reaction:



The resulting gas SO_2 is charged of fine particles. It passes through a dry purification section (cyclones and ESP precipitators), wherein the iron oxide is recovered in a cooler and then is discharged to a storage hall via a scraper conveyor. After this, the gas moves to the wet purification section, and then to the drying - absorption which alternates with conversion section, to produce the sulfuric acid. [1-3]. The storage hall is equipped with a water sprinkling system to settle airborne particles. But given the small particle size and its high temperature, sprayed water only makes the situation worse than it is. A state of art has denoted a plenty of available technologies as cyclones [4, 5], hydrocyclones [6], electrostatic separators ESP [7, 8], baghouses [9-11], wet scrubbers [12] etc. The integration of one of these equipments in the circuit will only improve slightly the collection efficiency, not cool and confine the dust particles. A rotating drum, based on the field of granulation [13-15], fitted with a water spray system will confine the dust and reduce its powdery aspect by moistening. But before designing the dusting system, it would be required to reduce the temperature of the iron oxide to not evaporate sprayed water.

A coil immersed into the bed of particles within the conveyor will allow efficient heat exchange [16, 17]. The aim of this work is therefore to demonstrate the point and applicability of this new combination of dust collection systems. The rotating drum is inspired from granulation field. But the particularity here is, instead of adding a binder to the granules, a water spray system will be integrated. These sprays consisted in atomizing water by special nozzles which produce a microscopic droplet mist along the drum. Moreover, water consumption will decrease. Furthermore, the exchange ratio between a suspension and a network of tubes depends on the physicochemical properties of both fluid and solid phases. It is generally situated between 200 and 600 W/(m².K) [18, 19].

The reason for such ability is due to the movement of particles into the bed. Each particle acts as a small reservoir of heat, which pumps easily the heat and moves within the fluid bed towards the wall of the exchanger. That is what justifies the technical interest that has often the heat transfer rate between a network of submerged pipes and a mixture of particles. Good heat transfer properties of these systems have led us to adopt them in this case where tight control of temperature is required.

2. Materials and methods

2.1. Dust cooling system design

One of the major obstacles to dust collection and confinement in this process is the high outlet temperature of hematite. Although the storage hall was equipped with a sprinkler system, it seems not effective. It is therefore appropriate to design the coil based on the lower dust outlet temperature. We set it at 50°C, with a water temperature variation from 25°C to 70°C. So, the system will be controlled and evaporation in the tubes will be avoided. The exchange surface is thus calculated. Afterwards, the coil disposition will be determined, taking into account the available space within the scraper conveyor where it will be incorporated. Figure (1) shows the procedure followed to design the coil:

2.2 Thermal design

Many heat transfer investigations between a fluidized system and a network of tubes were made, although the agreement between the correlations proposed by different workers is poor, with differences of one or even two orders of magnitude. These important deviations reasons seem to be related to the critical dependence of heat transfer coefficients to the geometry of the system, and its thermal properties to the flow type. In order to achieve the overall exchange coefficient, it was recommended to dissect the heat transfer sub-phenomena (Figure 2).

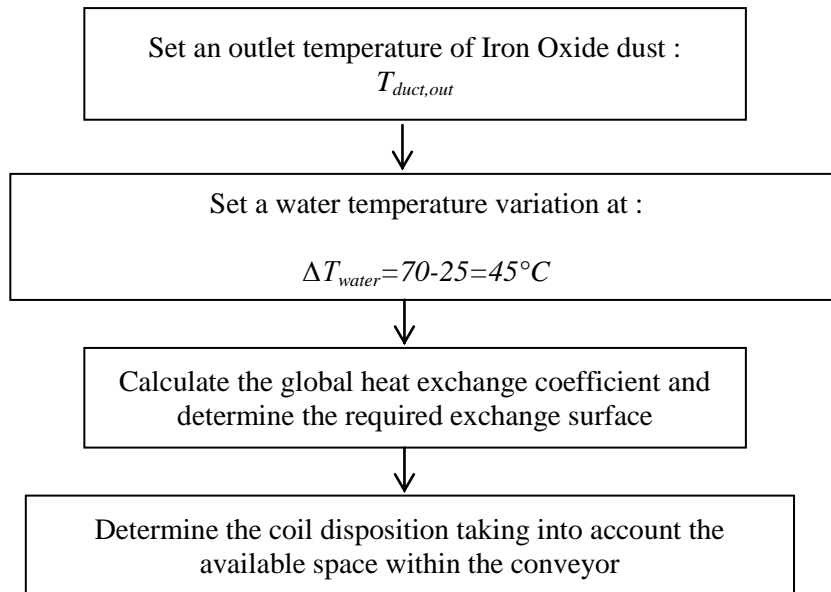


Figure 1: Organization chart of coil design

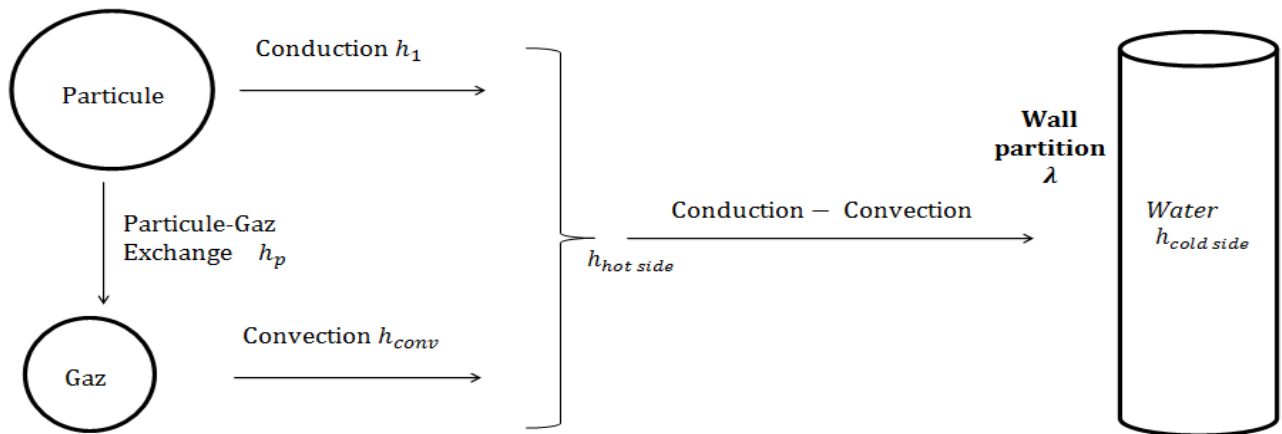


Figure 2: Diagram illustrating the different transfer modes

2.2 Thermal design

Many heat transfer investigations between a fluidized system and a network of tubes were made, although the agreement between the correlations proposed by different workers is poor, with differences of one or even two orders of magnitude. These important deviations reasons seem to be related to the critical dependence of heat transfer coefficients to the geometry of the system, and its thermal properties to the flow type. In order to achieve the overall exchange coefficient, it was recommended to dissect the heat transfer sub-phenomena (Figure 2). Certainly, the fraction of gas escaping with dust exchanges heat. However, it is still minimal since the exchange occurs as well within the upstream equipment. In addition, the particle is responsible of conduction and the gas of convection. The combined conduction-convection effect demanded targeted correlations. Equation (1) translating these exchanges will be identified clearly.

$$Q_{global} = U * S * DTLM = Q_{convection} + Q_{conduction} = Q_{hotside} \quad (1)$$

Or:

$$Q_{Hematite} = Q_{conduction} + Q_{particule - gas} \quad (2)$$

So by explaining each term, it follows the formula :

$$Q_{Hematite} = (h_{cond} * S_{particle-paroi} * \Delta T_{particule-paroi} + h_{particule-gas} * S_{particule-gas} * \Delta T_{particule-gas}) \quad (3)$$

And:

$$Q_{Hematite} = \dot{m}_{Hematite} * C_{Hematite} * \Delta T_{Hematite} \quad (4)$$

h_{cond} in Eq(3) is the conductivity term (λ/e) written in analogy form with convection terms.

The total quantity of heat exchanged is then deduced according to the variation of the temperature of the dust

$$Q_{global} = Q_{convection} + (Q_{Hematite} - h_{particule-gas} * S_{particule-gas} * \Delta T_{particule-gas}) \quad (5)$$

➤ Particle-gas exchange

The heat transfer between the particles and the gas may be compared to the gas convection from a single particle. A common definition of the transfer coefficient can be used based on the surface of a single particle ($a_p = \pi d_p^2$).

$$h_p = \frac{q}{a_p (T_p - T_g)} \quad (6)$$

The heat transfer coefficient between the particles and the gas is generally not large, particularly in this case where the amount of gas can be neglected. The h_p values for common applications are in the range of about 1 to 100 W/m².K. Experimental measurements of h_p were made by various researchers, among them, the equation presented by Kunii and Levenspiel (1969-1991) [19]:

$$Nu_p = 0.0282 Re_p^{1.4} Pr_g^{0.33} \quad (7)$$

Where:

$$Re_p = \frac{\rho_g U_g d_p}{\mu_g}; \quad Nu_p = \frac{h_p d_p}{\lambda_g}; \quad Pr_g = \frac{\mu_g C_{p,g}}{\lambda_g}$$

➤ Gas convection

Vreedenberg's (1958) [20] correlation in the case of horizontal pipes:

For $\frac{\mu_p}{\rho_p} Re_p \leq 2050$:

$$\frac{h_{conv} D_t}{\lambda_g} = 0.66 Pr_g^{0.3} \left(\frac{\rho_p (1-\varepsilon)}{\rho_g \varepsilon} \right)^{0.44} Re_D^{0.44} \quad (8)$$

Where:

$$Re_D = \frac{\rho_g U_g D_t}{\mu_g}$$

The value of the apparent porosity of the product to the velocity U is given by the correlation:

$$\varepsilon = \varepsilon_{mf} \left(\frac{Re_p + 0.02 Re_p^2}{Re_{mf} + 0.02 Re_{mf}^2} \right)^{0.1} \quad (9)$$

Where:

$$\varepsilon_{mf} = 0.586 * \theta_s^{-0.72} * Ar^{-0.029} * \left(\frac{\rho_g}{\rho_p} \right)^{0.021}$$

$$Re_{mf} = (33.7^2 + 0.0408 * Ar)^{0.5} - 33.7 \quad \text{and} \quad Ar = \frac{\rho_g (\rho_p - \rho_g) d_p^3 g}{\mu_g^2}$$

➤ **Exchange coefficient at the hot side**

In practice, the hot side coefficient h_c (including both conduction and convection) is directly correlated to the system settings. There is a huge number of correlations of this type, especially for heat exchange between the carried bed and a submerged tube network. Among the best, we can cite Dow and Jakob's correlation [18]:

$$\frac{h_c D_t}{\lambda_g} = 0.55 \left(\frac{D_t}{b}\right)^{0.65} \left(\frac{D_t}{d_p}\right)^{0.17} \left[\frac{(1-\varepsilon)\rho_p C_p}{\varepsilon\rho_g C_g}\right]^{0.25} \left[\frac{\rho_g U_g D_t}{\mu_g}\right]^{0.8} \quad (10)$$

➤ **Exchange coefficient at the cold side**

Within the tubes, the most commonly used formula is that of Mac Adams [16]:

$$Nu = 0.023 Re_{eau}^{0.8} Pr_{eau}^{0.4} \quad (11)$$

➤ **The global heat exchange coefficient**

Each one of the terms of the heat transfer being identified, the overall exchange coefficient is available.

$$Q_{global} = Q_{Hotside} = Q_\lambda = Q_{coldside} = U * S * DTLM \quad (12)$$

The overall heat exchange coefficient U depends on the distribution of the thermal resistance in the heat exchanger. Neglecting the thickness of the tubes, the heat exchange surfaces are equal for the two fluids, it follows that:

$$\frac{1}{U} = \frac{1}{h_c} + \frac{e}{\lambda} + \frac{1}{h_f} \quad (13)$$

➤ **The exchange surface**

According to the equation (5) and (12), and since h_{conv} is of the order of 10^{-3} , the term $(h_{conv} \cdot S_{gaz-paroi} \cdot \Delta T_{gaz-paroi})$ is negligible. And since the emerging gas and the dust particles are in equilibrium ($\Delta T_{gaz-paroi} \approx 0$), it follows that:

$$S = \frac{Q_{global}}{U \cdot DTLM} \quad (14)$$

The key of the coil disposition is the exchange surface required. Its calculation involves determining the overall exchange coefficient. Having all the necessary parameters except water flow velocity through the coil, it would be calculated indirectly in the heat exchange ratio. Initially, the value of the velocity is estimated to begin the iterative calculation. Another parameter that will be calculated at this level, is the quantity of heat exchanged and which is a function of the DTLM, the exchange surface and overall heat exchange coefficient. This heat will be transmitted to water. This way, finding the water flow required will be automatic. Given a standardized diameter of the coil tube, velocity will be deducted. If this latter is not too different from the velocity estimated, thermal specifications emerging from this calculation will be retained. Otherwise, the deduced velocity is instilled in the loop of the figure (3) until convergence.

Based on the margin diameters offered by Walraven company [22] in the case of steel tubes {10.2 ; 13.5; 17.2 ; 21.3; 26.9 ; 33.7 ; 42.4 ; 48.3; 60.3 ; 76.1; 88.9 ; 114.3 mm; ...}, the inner diameter is chosen, to which corresponds a thickness e and a nominal diameter DN .

2.3 Coil geometry

The exchange surface allows the determination of the total length in contact with the bed of particles. The next step is to determine the optimal design and the appropriate one due to the geometrical constraint: the available volume within the conveyor (Figure 4).

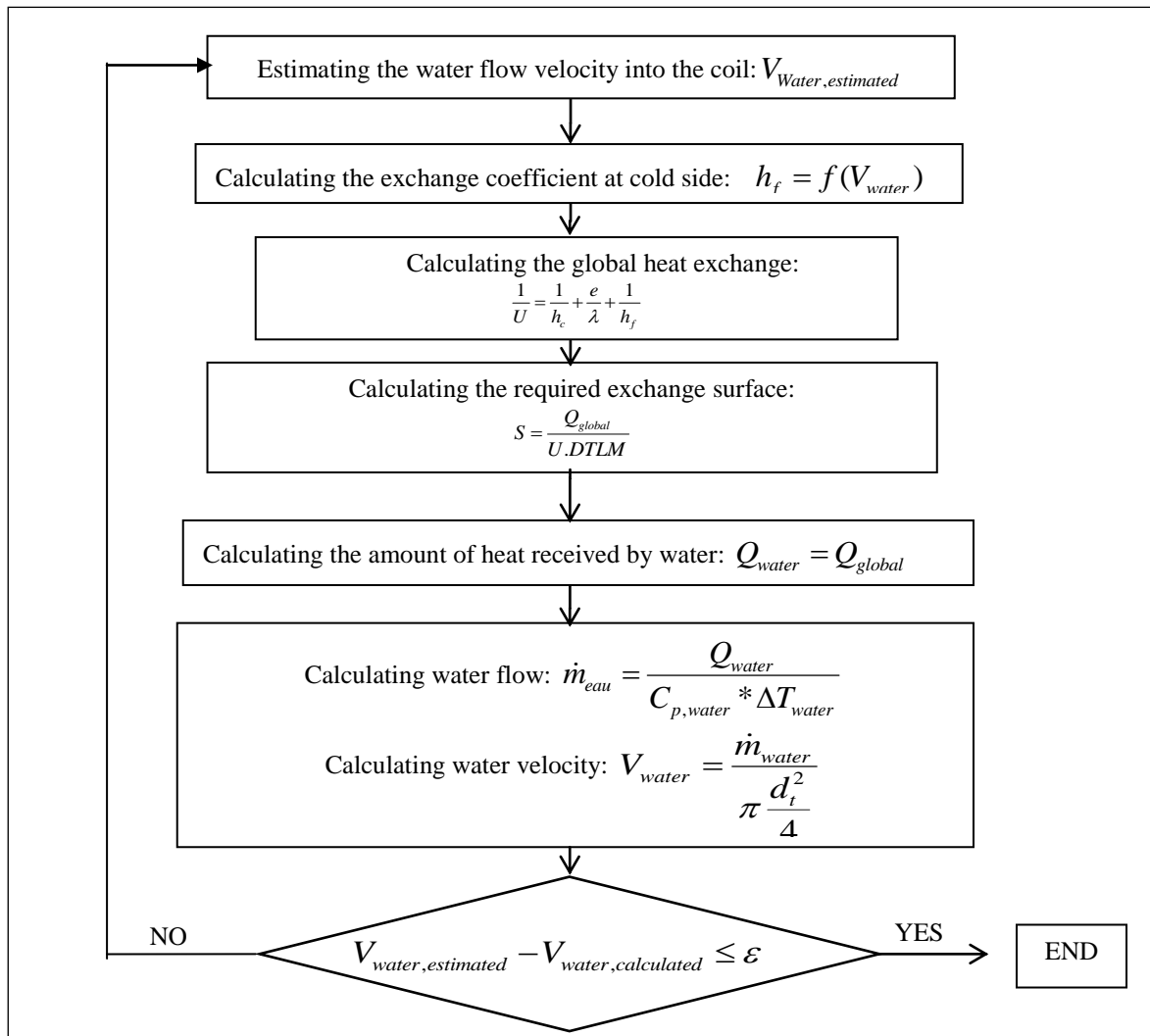


Figure 3: Thermal design procedure of coil

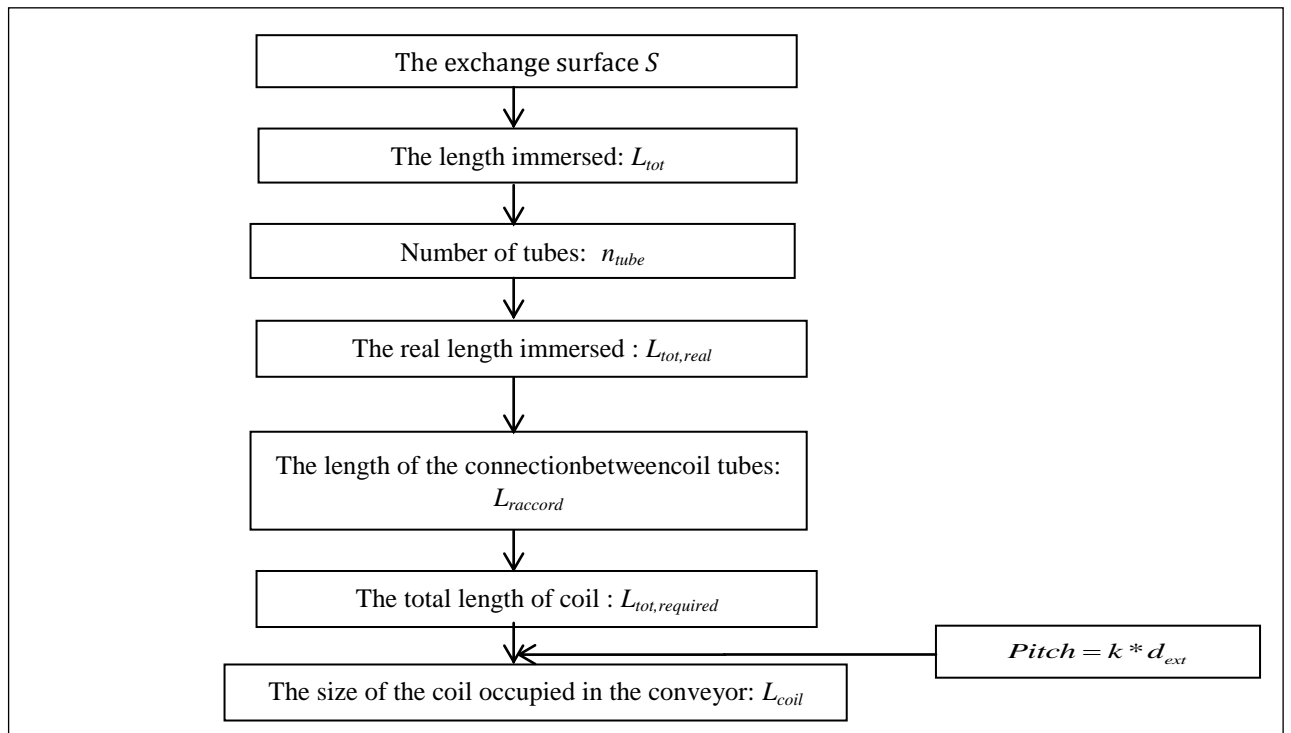


Figure 4: Organization diagram of the coil geometry determination

- The immersed length L :

$$S = \pi \frac{d_{ext}^2}{4} L_{immersed} \quad (15)$$

- Number of tubes n_{tube} :

$$n_{tube} = \frac{L_{immersed}}{L_{tube}} \quad (16)$$

Pitch :

With $1 < k < 2$

$$Pitch = k * d_{ext} \quad (17)$$

- The length of connections :

$$L_{connection} = 2\pi \frac{R_{moy}}{2} = 2\pi(d_{ext} + \frac{d_{ext}}{2}) / 2 = \frac{3}{4} \pi d_{ext} \quad (18)$$

- The total length required :

$$L_{tot,required} = L_{immersed} + (n_{tube} - 1)L_{connection} \quad (19)$$

- The coil length

$$L_{serpentine} = n_{tube} * d_{ext} + (n_{tube} - 1) * pitch \quad (20)$$

The above design parameters are shown in Figure (5)

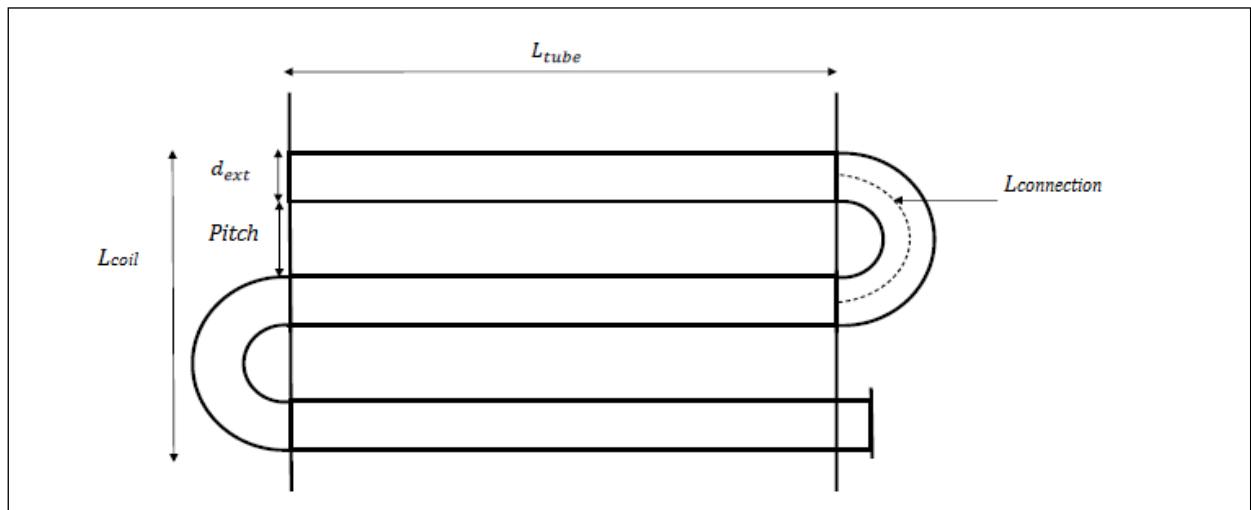


Figure 5: Scheme of the coil design

2.4 Rotating drum design

The dust being cooled, can be settled easily. Aiming the simplicity of technology, two solutions have been coupled: the rotating drum and a misting system. It consists of a rotating ring on supports, inclined a few degrees relative to the horizontal. The product is introduced to the uppermost side and progresses in the drum under the combined effect of rotation and tilt to be discharged at the opposite side. Although the construction methods of a rotating drum remains an industry secret, researches led to a key parameter, the speed of rotation. Indeed, there is a critical speed at which the solid particles do not slide, but rotates as a block with the cylinder. The rotational speed is usually set between 25% and 40 % of the critical speed, given by [12]:

$$n_{crit} = \frac{30}{\pi} \sqrt{\frac{2g}{D}} \quad (21)$$

The inclination, in turn, can only vary a few degrees between 2 and 10 degrees.

As detailed in the flowchart of Figure (6), the calculation process consists of opting for a drum diameter, which determines the range of variation of the rotation speed. The length of the drum will be determined by proportionality with the selected diameter. Similarly for an optimal speed, which guarantees homogenization of the powder with water, there is also a perfect fill rate. This rate depends greatly on the moisture content and load. In general, the filling ratio is from 20% to 40%. By setting the number of baffles, it will automatically result in the pitch between turns. At this stage, the rotational speed will be calculated as the flow rate of wet dust by volume delimited between two consecutive turns. This is the volume that will be evacuated by each turn. Since the calculation is iterative, the speed of rotation to be retained is the one that fits in the domain of variation previously determined. Specifically, it is the smallest value that will be adopted to avoid high electricity consumption, because rotation means also power consumption, and to reduce the space occupied by the equipment, because bigger the drum is, greater the wear will be enhanced between shell and roller.

In these conditions, and by analogy with the case of liquids, correlations "truncated" between two dimensionless numbers (usually the power number N_p and the Froude number Fr) are used. For a drum rotating around its axis of symmetry, a relationship between the Froude number and the Newton number Ne was found and tested on several devices by Sato et al. [13]:

$$Ne = A + BFr \quad (22)$$

$$Ne = \frac{T}{\rho g R^3 L} \quad (23)$$

$$Fr = \frac{RN^2}{g} \quad (24)$$

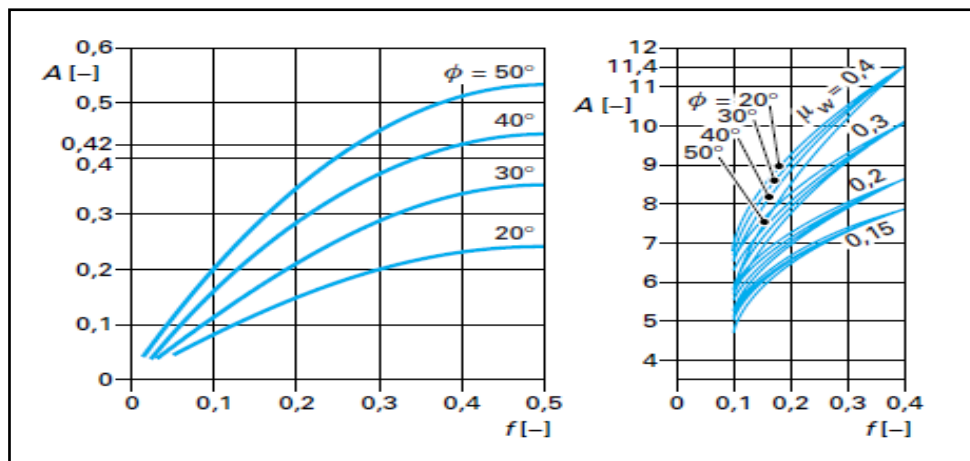


Figure 6: Design criteria of a rotary drum mixer [14]

2.5 Spray system design

➤ Saturation rate

The final solid grain quality depends greatly on the wetting liquid content contained in the pore volume. Newitt and Conway-Jones (1958) introduced in the study of the granulation a parameter called "saturation", denoted S , defined by the ratio of the volume of wetting liquid to the total volume of inter-particle pores [14].

$$S = w \frac{(1 - \varepsilon) * \rho_s}{\varepsilon \rho_l} \quad (25)$$

A required humidity of 15 % puts us in the funicular state. When the saturation rate exceeds 25%, the liquid droplets in the form of lenses coalesce and form a partial continuity of the inter-particle environment. The capture of dust is more effective when the dust particles collide with water droplets of similar size. Before consulting the nozzles Spraying Systems Co. contractor [23], a calculation draft was done according to the key parameters mentioned in their catalog (Figure 10). A wide variation of the spray angle ranging from 0 ° to 175 ° is provided. We started with the most common angle: 30 °.

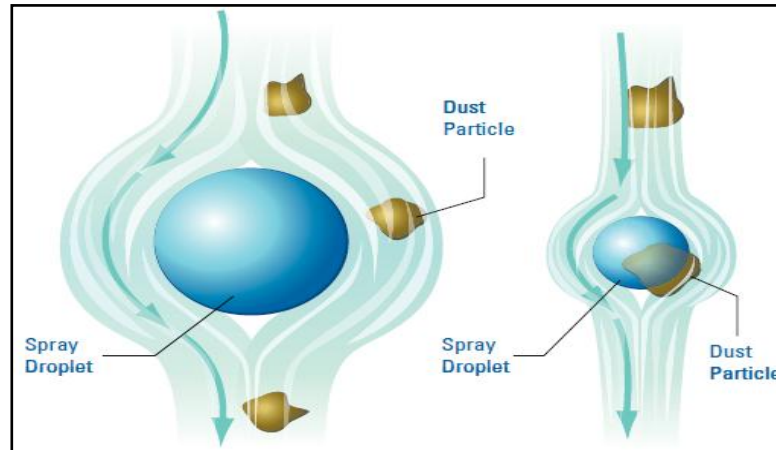


Figure 7: Size of water drop Vs dust particle

Figure (8) shows schematically the relationship between the spray angle and position of the nozzle. Having the diameter of the drum and the height of baffles, the height of the nozzles relative to the bed of dust particles will be calculated. This will be used to determine the distance covered by nozzle "coverage". The necessary number of nozzles will be determined by simple division of the drum diameter by "coverage". Since the water flow is detected from required humidity, the flow of water sprayed by nozzle will be deducted. Adopting a water flow velocity in the pipes no more than 3m/s, the diameter of the nozzle will be accessible.

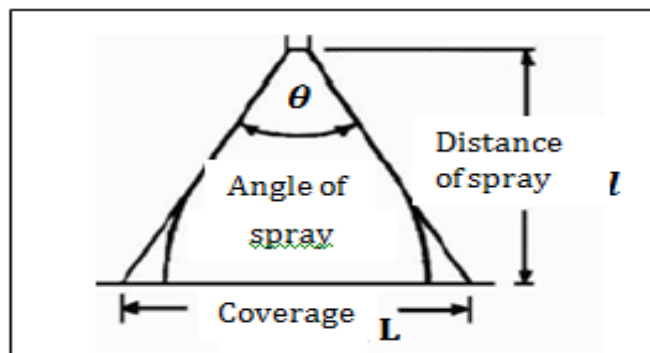


Figure 8: Diagram of the spray nozzle parameters

3. Results and Discussion

The choice of the internal diameter is not random. It is based on the heat exchanged which affords to cut down the outlet temperature of dust to 50°C. Any value that does not respect the constraint of the space allowed to the coil within the conveyor is rejected. Therefore, a coil with an exchange surface of 20.68 m² can be retained. The water flow rate through the coil is calculated based on the diameter of its tubes. The disposition of the tubes of coil is then figured out. (Table 1)

Table 1: The exchange surface according to the diameter and the water flow rate through the coil

$d_{int} (mm)$	$U (W/m^2.K)$	$S (m^2)$	$V_{water} (m/s)$
26.9	323.62	28,7	7.33
33.7	367.3	25.28	4.67
42.4	417.84	22.23	2.95
48.3	449.09	20.68	2.27
60.3	505.24	18.38	1.46
76.1	571.55	16.25	0.92

The desired degree of wettability was the key for the drum design and for the spraying system. With a filling rate of 20%, a residence time of 64.8 s and a spraying angle of 30°, the funicular state is reached:

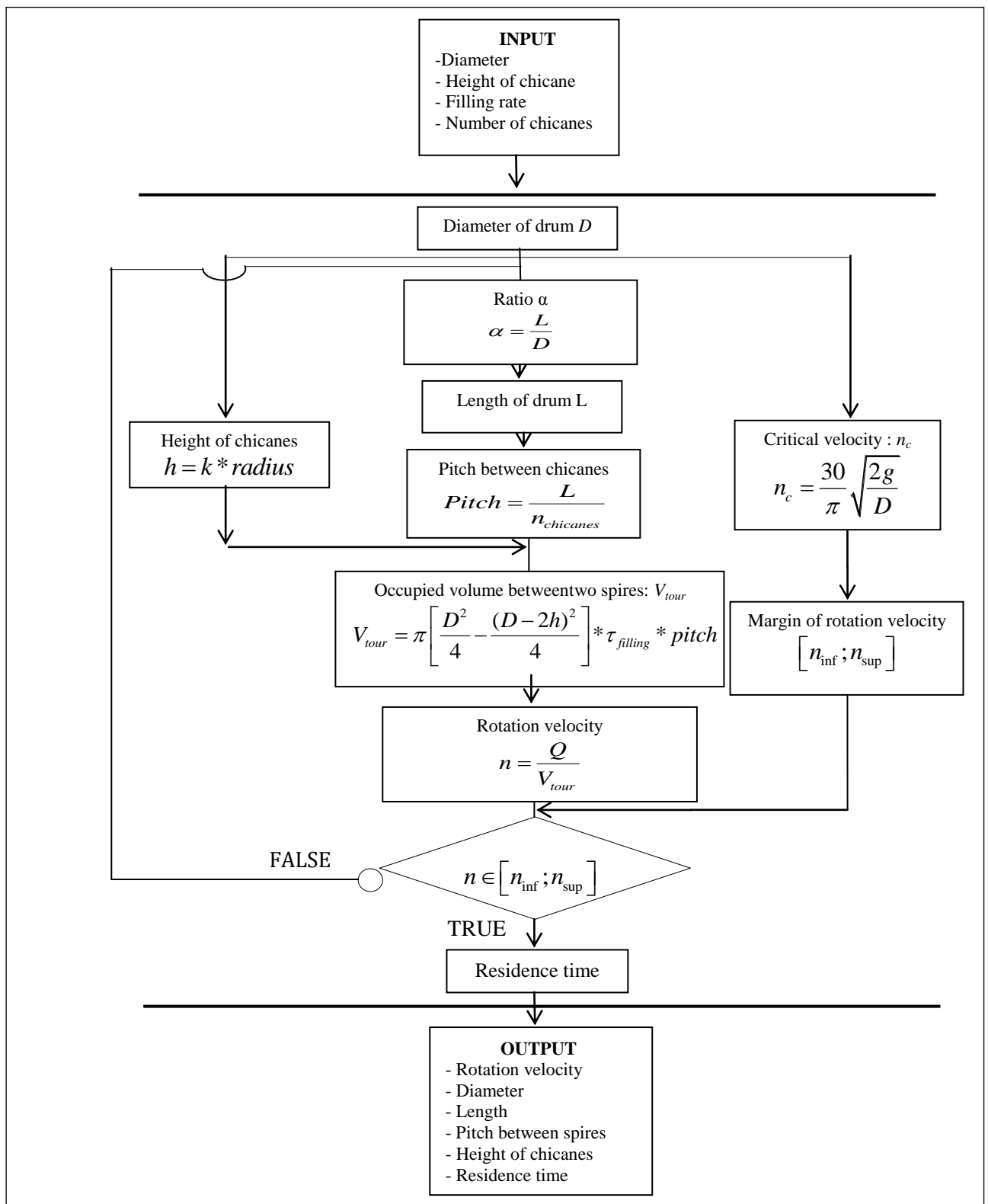


Figure 1: Design flow chart of the rotary drum

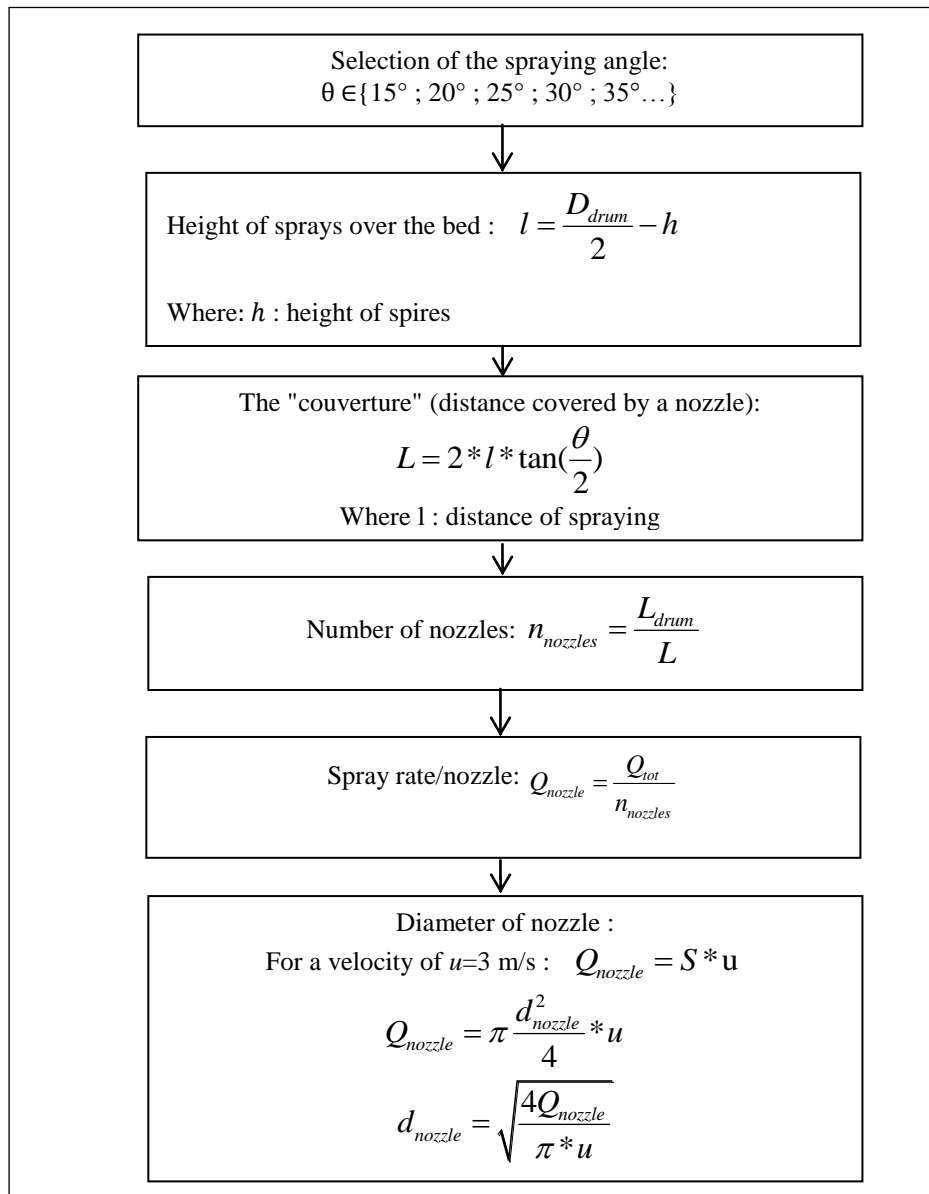


Figure 10: Design chart of spray nozzles

Based on velocity criterion, the selected internal diameter is 48.3 mm, corresponding to a thickness of $e=2.6$ mm and a nominal diameter of DN=40 mm. The results obtained are summarized in Table (2):

Table 2: The exchange surface according to the diameter

Inner diameter of coil	48.3	mm
Outside diameter of coil	53.5	mm
Thickness of coil	2.6	mm
Total length of coil	143.22	m
Number of tubes per stage	88	
Pitch	110	mm
The length occupied by coil	14.02	m
The height occupied by coil	17.6	cm
Water flow	15	m ³ /h
Water velocity inside tubes	2.27	m/s

Construction specifications of the cooling rotary drum are shown in table 3 below:

Table 3: Dusting system specifications

Drum	Dust rate (T/h)	30
	Diameter (m)	1.3
	Length (m)	2.3
	number of spires	9
	Pitch between spires (m)	0.26
	n (tr/min)	9.26
	Filling rate f	0,2
	Height of chicanes (m)	0.15
	Residence time (s)	64.8
	Tilt (°)	5
	P (KW)	15.5
Sprays	Spraying angle	30
	Number of nozzles	9
	Distance between nozzles and bed (m)	0.5
	Flow rate of nozzle (m ³ /h)	0.6
	Nozzle diameter (m)	0.0085
	Spraying velocity (m/s)	3

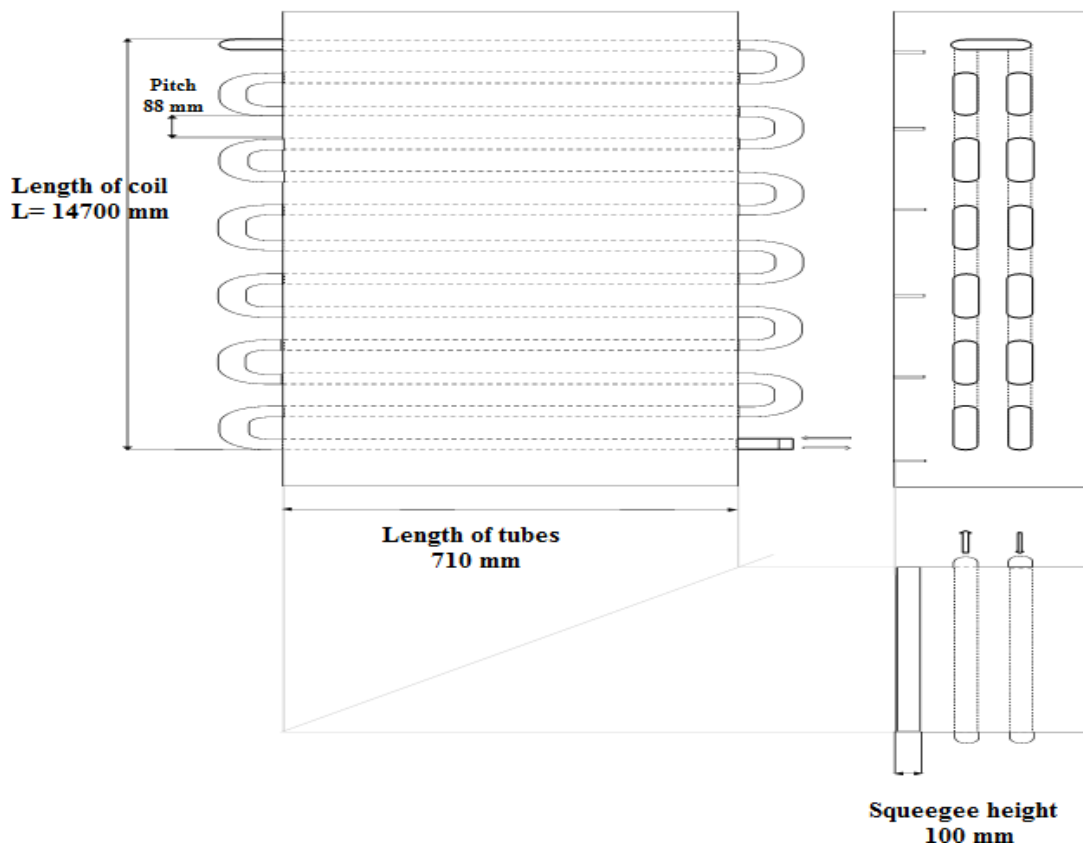


Figure 11: Drawing specification of coil

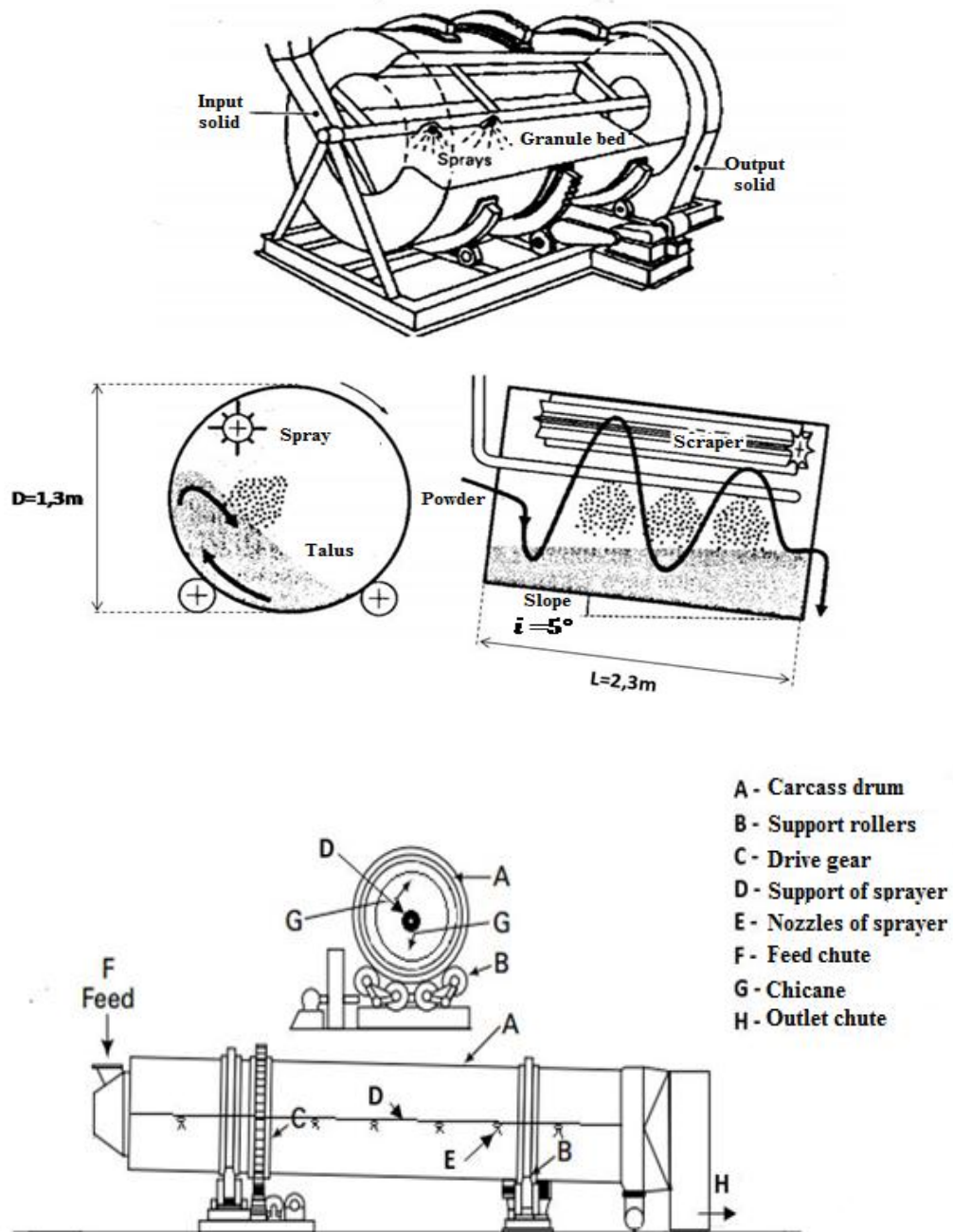


Figure 12: Specifications diagram of rotary drum with a spray system

Conclusions

The proposed dust removal system consists of a coil and a rotary drum with sprays. The coil immersed in the bed of fine particles transported in the conveyor, provide an outlet temperature of $60^\circ C$ down from $270^\circ C$. This pretreatment will greatly facilitate the task of the drum. A rotary drum for which the design was inspired from the granulation field, will contain airborne dust; while the integrated system of nozzles will handle dust by abating due to water atomization. This will enhance sensibly dust particles settling.

For the sulfuric acid plant, taken as case study, as a significant part of its budget is allocated to Fe_2O_3 logistics, especially the removal of this by-product from the overstocked storage hall to the outer waste dikes with large amounts of water spraying to ensure the humidity required, the system developed in this study will save these expenses and eradicate the problem of airborne dust. This system can also be used in similar plants and in other plants with dust problems not efficiently handled with conventional technologies.

References

1. Hu G., Dam-Johansen K., Wedel S., Hansen J. P., *Prog. Energy Combust. Sci.* 32(3) (2006) 295.
2. Marcos L.S. Oliveira., Colin R. Ward., Maria Izquierdo., Carlos H. Sampaio., Irineu A.S. de Brum., Rubens M. Kautzmann., Sydney Sabedot., Xavier Querol., Luis F.O. Silva., *Sci. Total Environ.* 430 (2012) 34.
3. I Alp., H Deveci., E.Y Yazıcı., T Turka., Y.H Sungun., *J. Hazard. Mater.* 166 (2009) 144
4. Wu K., Liu G., Mo Y., *Powder Technol.* 295 (2016) 1.
5. Gimbun J., Chuah T. G., Choong T. S., Fakhru'l-Razi A., *Int. J. Comput. Methods Eng. Sci Mech.* 6(3) (2005) 161.
6. Mai Manga M., Bazin C., Renaud M., *Can. Metall. Q.* 51(2) (2012) 126.
7. Porteiro J., Martín R., Granada E., Patiño D., *Fuel Process. Technol.* 143 (2016) 86.
8. Jędrusik M., Świerczok A., Air Pollution–Monitoring, Modelling, Health and Control” Intech, 2012. (Chapter 9).
9. Strobos J. G., Friend J. F. C., *Hydrometallurgy.* 74(1) (2004) 165.
10. Siret, B., *Techniques de l'Ingénieur.* J3580 (2001).
11. Couper J. R., Penney W. R., Fair J. R., Chemical Process Equipment, Selection and Design, Gulf Professional Publishing. (2009).
12. Bouziani A., Maalmi M., Tahiri, M., *C R Phys.* 7(2) (2006) 293.
13. Khashayar S., Guigon P., *Techniques de l'Ingénieur.* J 2254 (2009).
14. Berthiaux H., *Techniques de l'Ingénieur.* J 3397.
15. Boudiaf Y., Nancy: Université Henri POINCARÉ. 82 (2009).
16. Puttewar A. S., Andhare A. M., *Int. J. Res. Eng. Technol.* 4 (2015) 416.
17. Bennajah M., Chaouni N., ECHANGEURS DE CHALEUR : Technologie, calcul et design, Editions T. 2014.
18. Wen-Ching Y., Handbook of Fluidization and Fluid-Particle Systems, Siemens Westinghouse Power Corporation, Pittsburgh, Pennsylvania, U.S.A., Marcel Dekker, Inc., 2003
19. Coulson J., Richardson J., Chem. Eng: Chem biochem. react. Proc. control. 3 (1994).
20. Kunii D., Levenspiel O., Fluidization Engineering. (1969).
21. Vreedenberg H. A., *Chem. Eng. sci.* 9(1) (1958) 52.
22. Data sheet Pipe Dimensions and Weights (EN). 07/2015.
23. Spraying Systems Co. Experts in Spray Technology. A Guide to Spray Technology for Dust Control. 2016.

(2017) ; <http://www.jmaterenvironsci.com>